CEAS Aeronautical Journal (2021) 12:573–587
https://doi.org/10.1007/s13272-021-00519-5

ORIGINAL PAPER

Production and characterization of experimental low noise trailing edges made of cold rolled porous aluminum with special attention to the influence of cold rolling on the mechanical stability of the investigated materials

Jörn Tychsen[1] · **Joachim Rösler**[1]

Received: 24 April 2020 / Revised: 14 May 2021 / Accepted: 18 May 2021 / Published online: 31 May 2021

Abstract
In the framework of the CRC 880 "Fundamentals of high-lift for future civil air craft" methods for the reduction of aircraft noise are investigated. An important method for this noise reduction is the usage of porous material as low noise trailing edges. To improve the aeroacoustic properties of porous materials, an innovative rolling process was established by Tychsen et al. (Metals 8:598, 2018). Here, the rolling process is described as it is used as an important method for the production of samples. The influence of cold rolling on two different porous materials namely porous aluminum 80–110 (PA 80–110) and PA 120–150 is investigated. Important characteristics studied are the porosity, mechanical properties and the dependence of flow resistivity from the degree of deformation. The flow resistivity is of particular interest as the aeroacoustic performance is significantly influenced by it. The results are then compared to the findings for PA 200–250, which was investigated in Tychsen et al. (Metals 8:598, 2018). Lastly, experimental trailing edges made out of cold rolled porous aluminum with a gradient in thickness reduction are shown. The characterization of the aeroacoustic behavior is not part of this study. Reference is made to Rossignol et al. (Int J Aeroacoust 19:365–384, 2020), where trailing edges shown here are characterized aeroacoustically. The findings shown here demonstrate that different porous materials can be tailored by cold rolling without negative impact on the mechanical behavior. It is proven that the new rolling process is a versatile tool for the production of gradient porous material.

Keywords Porous aluminum · Cold rolling · Trailing edge porosity · Mechanical behavior

1 Introduction

The CRC 880 investigates methods for reducing aircraft noise. By using increasingly quieter engines, the sound generated by the turbulent flow around the wings becomes more important, especially during landing. An elementary source mechanism lies at the trailing edge of the wing when the vortex structures of the turbulent boundary layer interact with the sharp trailing edge of the wing profile. At the discontinuous transition from wall-bound to free flow, an acoustic signal is generated by each vortex. Porous materials can be used to reduce this signal. With their permeability, these materials allow communication between the flow on the upper and lower wing surface, which has been proven to be elementary for the acoustic effect in different studies (e.g. compare [3–11]). Porous materials soften the aforementioned discontinuity of the trailing edge. First tests in the acoustic wind tunnel (AWB) of the DLR in Braunschweig as well as simulations with different materials showed promising results, especially for a porous aluminum (PA) produced by a salt infiltration technique [1, 9, 12, 13].

Rossian et al. [14, 15] showed, using acoustic simulations, that an optimized porous material should have locally different flow resistivities. This can be seen in Fig. 1, where the de-dimensionalized fluctuating sound pressure (fluctuating sound pressure divided by linearized dynamic pressure of the disturbance field of the vortex - to be independent of the test vortex used, compare [16]) generated by a single vortex passing over the wing surface is the ordinate value. The abscissa shows a time interval. Within this interval, the simulated vortex passes the junction of non-porous to porous

✉ Jörn Tychsen
j.tychsen@tu-braunschweig.de

[1] Institute for Materials Science, TU Braunschweig, Langer Kamp 8, Braunschweig 38106, Germany

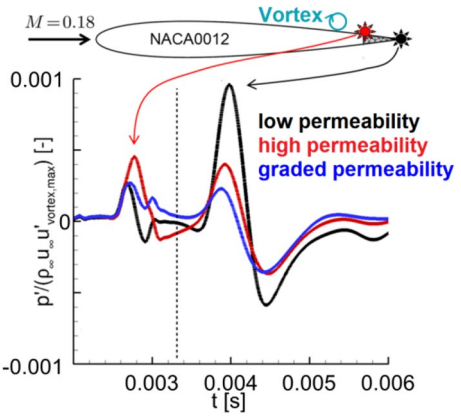

Fig. 1 Results of acoustic simulations showing the effect of using graded porous material (blue line) compared to uniform porous material (red line, black line) as a low noise trailing edge (adapted from [14])

material as well as the actual trailing edge, reaching the area of free flow. Using the time and the velocity of the vortex, the two local peaks can be assigned to the point of attachment of the porous material insert on the one hand and to the actual trailing edge on the other. This is a clear indication that an additional source is generated at the junction of non-porous to porous material. By using a highly permeable material (i.e. low flow resistivity, red curve) the peak at the trailing is reduced, whereas the peak at the point of attachment increases. Thus, the resistivity needs to be high at the transition from the non porous part of the wing to the porous material and very low at the actual trailing edge at the end of the wing (compare blue line in Fig. 1). A gradual transition between the impermeable wing surface and free flow is to be achieved, to reduce both noise sources. Such a smooth transition was also shown to be beneficial by Rubio Carpio et al. [17] and Schulze and Sesterhenn [18].

The simulations performed by Rossian et al. [14] are based on a set of volume averaged perturbation equations introduced by Faßman et al. [19] as well as a set of acoustic interface conditions by Rossian et al. [20]. The volume averaged pertubation equations are used to reduce the computational effort for simulating the acoustic problem. Using them, it is not necessary to resolve the acoustics inside the porous material. Instead, the porous volume is described using the parameters porosity, permeability and the Forchheimer coefficient [19]. Since indications for favorable design of porous inserts with respect to flow resistivity and porosity could be obtained from Rossian's simulations, these two parameters are of particular interest in this study. For a detailed description of the simulations, reference is made to [14, 15, 19, 20].

Ali et al. [4] found different relevant source mechanisms for permeable media, which show that other parameters, such as surface roughness, tortuosity (a measure of the tortuosity of the passages within a porous material) or pore size are of relevance for noise reduction or additional generation of noise. This is confirmed by the investigations of Kisil et al. [5] who examine the influence of the pore size in more detail. Furthermore, Devenport et al. [21] analyze and show the influence of surface roughness on acoustic scattering.

Note, that a main effort of the research within the acoustic part of the CRC 880 is to provide basic principles for the design of aeroacoustically optimized porous trailing edge inserts. Therefore, a reduction to the aforementioned parameters (porosity and flow resistivity/ permeability) is considered a good initial approach, especially since flow resistivity was identified as an parameter of main importance in other studies [7, 22–24].

In this article no evaluation of aeroacoustic wind tunnel measurements is carried out. The focus is on the materials science evaluation of the novel rolling process carried out for PA materials. The analysis of wind tunnel tests of the materials shown here is described by Rossignol et al. [2]. The results discussed by Rossignol et al. indicate that there is a need to further clarify correlations between noise reduction potential and material properties. Further analysis of the trailing edges shown here is therefore essential. Due to the gradient in thickness reduction, this task is not fulfilled easily and needs additional research. The surface roughness for example varies with the pore size as well as the tortuosity. Both parameters are changed during rolling. This is another reason, why the research within the CRC initially concentrated on porosity and flow resistivity as material parameters.

To achieve the aforementioned gradual transition from non porous to porous material, a rolling process was established within the framework of the CRC 880. A similar rolling process is mentioned in [25]. It was used to produce a thickness profile adapted to the actual material load [25, 26]. In the study shown here, the aim was to roll material with a gradient in thickness reduction in such a way that the requirements for a low noise trailing edge insert (compare [9, 14]) can be achieved. This rolling process was presented in [1] using a porous aluminum with a filter fineness in the range of 200-250 μm (PA 200-250) with a pore size ranging from 0.63 to 3 mm. The filter fineness describes the size of the link between pores within the material. The term filter fineness is described in Sect. 2.1 in more detail. In [1] the porosity, the flow resistivity and the mechanical behavior under quasi-static tensile load of cold rolled PA 200–250 are also characterized.

To further research the mechanism of noise reduction at the trailing edge, it is necessary to test different materials. In particular, the effect of a porosity gradient is to be further investigated using different materials. Therefore, the applicability and effect of the rolling process on two

other materials, namely PA 80–110 and PA 120–150, was investigated.

In the following, the material, the rolling mill and the production of uniformly rolled samples as well as samples with a gradient in thickness reduction is presented. The production of uniformly rolled samples is indispensable for the material characterization, since a characterization of properties apart from porosity is not possible with samples with a gradient in thickness reduction. The first step is to identify meaningful degrees of deformation. On the one hand, high-resolution computed tomography in conjunction with a defect-detection is used to determine porosity. On the other hand, quasi-static tensile tests provide information on the dependence of the mechanical properties from the degree of deformation. In connection with the porosity determination the influence of the increase of load-bearing material due to compaction during rolling can be deduced. In this way, material damage caused by the rolling process can be identified. This procedure was already described and used in [1, 27]. It is described here again as an important method. The results of the flow resistivity measurements are presented to conclude the investigations of uniformly rolled samples. After presentation of these results, computed tomography scans of experimental trailing edges made out of graded porous material are shown. The results obtained in this study are compared and evaluated with those shown for PA 200–250 in [1]. A further analysis of the flow resistivity of trailing edges rolled with a gradient in thickness reduction is not shown here due to space reasons but described in [28].

Note, that results of aeroacoustic measurements of the trailing edges are shown in [2]. Rossignol et al. are also using a perforated sheet metal with a gradient in porosity and flow resistivity with an non-periodic designed structure, which is compared to the TEs (trailing edges) made out of porous aluminum.

2 Methods

2.1 Materials

The porous aluminum used is purchased (from Exxentis AG). It is produced by infusing a placeholder structure of sodium chloride particulates with molten aluminum. After casting, the particulates are washed out. Thus, the pore size and the size of the link between pores correspond to the size of the sodium chloride particulates used for casting. In this way, the filter fineness is adjusted. The filter fineness is used to name the materials.

In this study material with a filter fineness in the range of 80–110 μm, (and a pore size in the range of 0.35–1.00 mm) named PA 80–110, and with a filter fineness in the range of 120–150 μm, (and a pore size in the range of 0.63–1.60 mm) named PA 120–150 is used. The filter fineness describes the maximum particle size that can pass through a filter material. The manufacturer uses the specification to classify his materials. In Fig. 2, these different materials (as received) are shown in a computed tomography reconstruction. Additionally, PA 200–250 which was used in [1] is shown in Fig. 2. The difference in pore sizes can be seen very well. Note, that the pore sizes for the materials are much taller than their filter fineness. This is due to the fact, that the links between pores are responsible for the filtering effect. These connections between the pores result from contact surfaces of the individual grains of the sodium chloride pack. These areas are considerably smaller than the pores themselves. Therefore the filter fineness is considerably smaller than the pore size. As in [1], material made out of technically pure

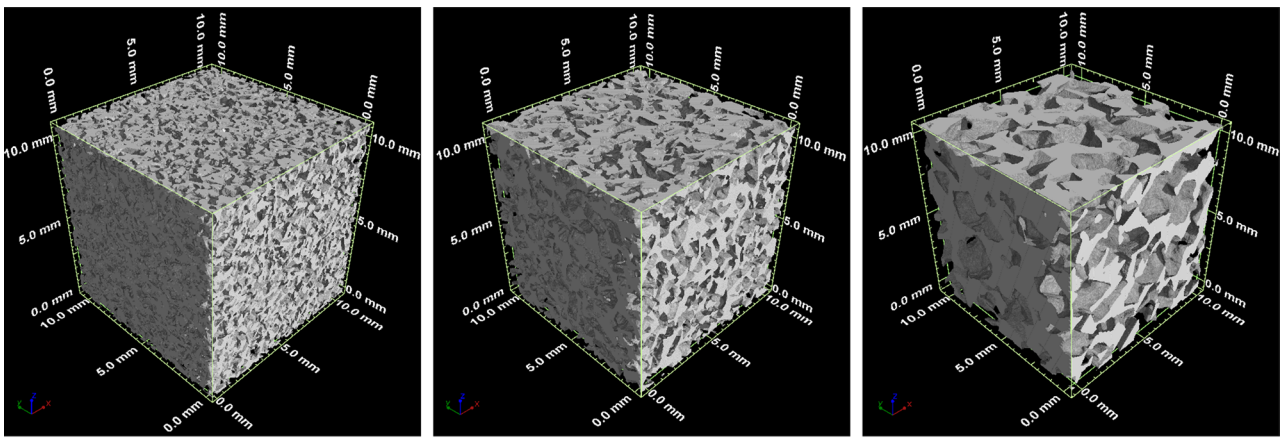

(a) PA 80-110 (b) PA 120-150 (c) PA 200-250

Fig. 2 Computed tomographic scans of the different materials used

aluminum A85 (according to GOST "The Russian Federal Agency for technical regulation and metrology") is used to ensure good formability during cold rolling.

The material is received in 500 mm x 300 mm size plates with a thickness of 20 mm. For rolling, samples are cut from the plates with a band saw in different dimensions. Samples used for flow resistivity measurements were 100 mm x 100 mm before rolling, samples used for mechanical testing were 100 mm x 125 mm before rolling and samples for production of experimental trailing edges were 100 mm x 250 mm before rolling. After rolling the material was further processed. This is described in the following sections.

Note, that different batches of PA 120–150 and PA 80–110 were used in this study. This is important, because the porosity of the material as received may vary due to minor variations during manufacturing. One batch was used for material characterization of porosity and mechanical behavior (Sects. 3.1 and 3.2). The porosity as received is $\Phi \approx 61\%$ for PA80–110 and $\Phi \approx 60\%$ for PA120–150. For the production of the experimental trailing edges material with porosity as received of $\Phi \approx 52\%$ for PA80–110 and $\Phi \approx 57\%$ (Batch17) and $\Phi \approx 62\%$ (Batch18) for PA120–150 was used. The flow resistivity measurements shown here were conducted using another batch. Despite different batches, a comparison of data is very well possible. This is due to the fact that for characterization of each parameter, such as flow resistivity, the same batch is used in each case. For the evaluation, the change of the parameters due to rolling rather than the absolute values is then in the forefront.

2.2 Rolling experiments

The rolling process for the production of graded porous material was firstly described in [1]. It is shown here again, because it is used as an important method. The rolling mill used is shown in Fig. 3. The special feature of the rolling mill is the hydraulically operated pull out table. This can be seen very clearly on the left side of the rolling mill below the monitor. For rolling of a gradient, the porous material is restrained on the pull-out table. The pull-out table provides exact position-information of the rolling stock in relation to the center of the rolling gap. This position information can be used to control the rolling gap as a function of the position of the rolled sample. This position information enables the rolling gap to follow programmed contours during the rolling process.

Rolling is performed with a duo roll set up with a rolling speed of 5 mm/s. The roll diameter is 200 mm and the roll width is 200 mm. The rolling force varied during the experiments from <1 up to 100 kN. It depends on the samples width as well as the thickness reduction per pass. Due to the reduction of porosity and work hardening, rolling force

Fig. 3 400 kN cold rolling mill with hydraulically operated pull out table

increases at high degrees of deformation. The samples for flow resistivity characterization and for mechanical testing were rolled uniformly.

The flow resistivity samples were rolled according to five locations of the "standard" gradient (Table 2). They are located at 0, 7.5, 15, 22.5 and 30 mm of the gradient length. A thickness of 18, 16, 14, 12 and 10 mm results at those locations after five passes of rolling. As with the trailing edge, the flow resistivity samples were rolled to the final thickness in five passes. The thickness reduction per pass corresponds to the thickness reduction at the aforementioned five locations during gradient rolling.

The samples for mechanical testing were rolled with a thickness reduction of 1 mm per pass. The number of passes thus results from the final thickness of the sample to be achieved.

The graded experimental trailing edges are usually rolled in five passes each. Each pass consisted of several steps. At first, the gap between rolls opens up to a value >20 mm so that the material can be inserted into the gap. In the next step, the gap is closed until the reduction per pass for the first area (left hand side in Fig. 4) is reached. Then, the rolls start to rotate and the pull out table moves into the direction of rolling. The pull out table pulls the sample with a small, constant tension. As soon as the beginning of the second area (mid in Fig. 4) is reached, the gap between rolls closes

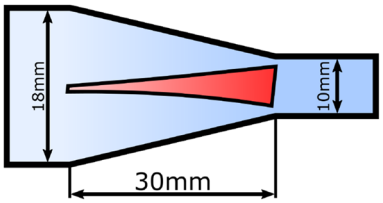

Fig. 4 Cross section of graded rolled sample with "standard" gradient, compare [1]

Table 1 "Light" gradient: gap between rolls during each pass for each area

No. of pass	First area: uniform / mm	Second area (30 mm): linear gradient / mm→ mm	Third area: uniform / mm
1	20.00	20.00→18.60	18.60
2	20.00	20.00→17.30	17.30
3	20.00	20.00→16.10	16.10
4	20.00	20.00→15.00	15.00
5	20.00	20.00→14.00	14.00

while the table and the rolls are still moving. This way, a linear gradient is rolled into the material until the beginning of the third area (right hand side in Fig. 4) is reached. In this area, the gap between rolls is kept constant until the whole sample leaves the gap. Later on, the process starts again with the first step. It is possible to enlarge the number of areas so that different linear gradients can be rolled into the material. Using the maximum number of areas, it is possible to roll a curve-like shape consisting of various linear gradients into the material. The gradients used in this study are shown in the Tables 1, 2 and 3.

The first experimental trailing edges were made out of cold rolled material with the "standard" gradient according to Table 2 [1]. To improve the understanding of the influence of graded porosity on the noise reduction potential two other gradients (Tables 1, 3) were investigated. The wing segment used in the aeroacoustic experiments has a thickness of 6.5 mm at the location were the porous trailing edge is attached to. Thus, the experimental trailing edge thickness needs to be 6.5 mm at the joining edge as well. The experimental trailing edges (colored in red in Fig. 4) are worked out of the graded samples as shown in Fig. 4. The gradient can be adjusted (colored in light blue in Fig. 4), but the geometry of the experimental trailing edge must be unchanged. Thus, the gradient in Table 3 is the gradient with the maximum degree of deformation in the third area (right hand side in Fig. 4) possible for material with a starting thickness of 20 mm. This is the reason why it is called "maximum" gradient in this study. The gradient itself could, of course, be further intensified by maintaining the initial thickness (20mm) in the first area (left hand side in Fig. 4),

Table 2 "Standard" gradient: gap between rolls during each pass for each area [1]

No. of pass	First area: uniform / mm	Second area (30 mm): linear gradient / mm→ mm	Third area: uniform / mm
1	19.60	19.60→17.40	17.40
2	19.21	19.21→15.13	15.13
3	18.82	18.82→13.17	13.17
4	18.45	18.45→11.45	11.45
5	18.00	18.00→10.00	10.00

Table 3 "Maximum" gradient: gap between rolls during each pass for each area

No. of pass	First area: uniform / mm	Second area (30 mm): linear gradient / mm→ mm	Third area: uniform / mm
1	19.70	19.70→17.60	17.60
2	19.40	19.40→15.30	15.30
3	19.10	19.10→13.20	13.20
4	18.80	18.80→11.20	11.20
5	18.50	18.50→9.40	9.40
6	18.25	18.25→7.90	7.90
7	18.00	18.00→6.50	6.50

like it has been done for the light gradient. However, this has not been tested in the studies carried out. Because of the major overall thickness reduction for the "maximum" gradient (Table 3), it is rolled in seven passes to limit the degree of deformation during each pass.

After rolling, the trailing edges are worked out of the graded rolled material by electrical discharge machining. This method is used to ensure a constant high quality with open pores for the complex and costly measurements in the acoustic wind tunnel. The geometry is shown colored in red in Fig. 4.

2.3 Material characterization

A CT scanner (GE nanotom s, GE Sensing & Inspection Technologies GmbH, Wunstorf, Germany) with a minimum possible voxel size of 0.5 μm was used for material characterization. The porosity determination was conducted using three-dimensional CT reconstructions with the defect detection of VG Studio Max 2.1 (by VolumeGraphics, Heidelberg, Germany).

The samples for porosity measurement (values in Fig. 7) were measured with the X-ray tube being operated at 80 kV acceleration voltage and 240 μA current using a 0.1 mm Copper filter. The detector was operated with an exposure time of 1000 ms. The samples were rotated 360° around their own axis. Images were saved every 0.25° averaging three images, resulting in a total of 1440 gray scale images. A skip

time of 1000 ms after each saved image was used. The voxel size was 13.75 μm/voxel.

Settings for the X-ray tube for measuring the experimental trailing edges (Sect. 3.3) were 90 kV acceleration voltage and 230 μA current together with a 0.1 mm Copper filter. The detector was set to an exposure time of 750 ms. The samples were rotated 360° around their own axis. Images were saved every 0.25° averaging three images, resulting in a total of 1440 gray scale images. A skip time of 750 ms after each saved image was used. The voxel size was 17 μm/voxel.

The experimental trailing edges were subdivided into six different Regions Of Interest (Region of Interest, ROI) to determine the porosity within the gradient that was rolled into the material. This procedure is described in [1] as well and is shown here in Fig. 5. In the direction of the thin end of the trailing edge, the analyzed volume decreases. However, the volume analyzed is sufficient for the determination of a reliable porosity value. As there is only one sample per state analyzed, no standard deviation is given for the porosity values in Table 5.

Tensile testing was performed with samples designed according to DIN 50125 form E. Though, an adaption has been made in the measuring length and the overall length of the samples. This adaption was made to be able to analyze the damage behavior of the samples with computed tomography during interrupted tensile testing. The corresponding CT measurements regarding the damage behavior are to be evaluated and are not part of this study. A similar sample design was used in [1] except that the length of the measurement zone and the overall length of the sample are different. The schematic diagram of the samples according to DIN 50125 is shown in Fig. 6. The associated dimensions used in this study are given in Table 4.

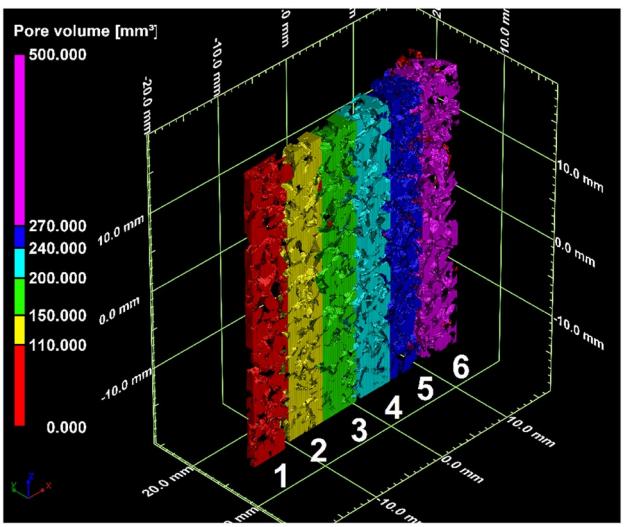

Fig. 5 Experimental trailing edge, subdivided into six regions of interest for porosity measurements (compare to [1])

The samples were worked out of the rolled material by cutting the rolled plates with a band saw. A minimum distance of 10 mm from the lateral edges to the measuring range of the samples was ensured. In this way, four samples could be obtained from each rolled plate, which were milled to the final sample dimensions. The samples were cut out of the middle of the material. During milling, the pores on the surface are smeared. This does not influence the determination of mechanical properties, since the material brought in does not take over a load-bearing function [30]. For the values given, three samples for each state were measured.

Besides porosity measurements and mechanical testing, flow resistivity measurements using the alternating air flow method (according to Method B DIN EN 29035 [31]) were performed. The uncertainty of this method is around 14 %. This uncertainty is not taken into account for the values given here. Within the investigations, the uncertainty of 14 % could not be reflected within the measurements carried out. The values given in Fig. 9 contain an uncertainty which is the result of multiple measurements (by different persons at different days) of one sample for each rolling state and each material.

The flow resistivity samples were extracted from the rolled plates using a cutting machine. The dimensions of samples are 80 mm $\times$ 80 mm $\times t$, where t is the thickness after rolling. Thus, a correction for non-standard sample sizes had to be applied [32]. Also in this procedure the lateral surfaces of the samples are smeared. This is not relevant for the flow resistivity measurement, as this is carried out perpendicular to the smeared surface. Furthermore, the lateral surfaces must be masked for measurement anyway.

The aeroacoustic behavior depends on the communication between the flow on the upper and lower wing surface. Thus, flow resistivity is an important parameter characterizing the aeroacoustic behavior, because it describes how easily air can flow through the material. However, the values given here refer to rolled samples as a whole, which are generally used to evaluate the change caused by rolling. The flow resistivity of similarly rolled trailing edges can, however, deviate considerably from the values given here, as the trailing edges are machined out of the material. This difficulty

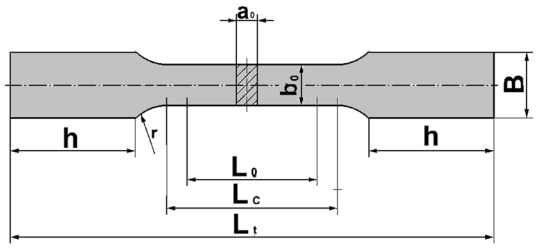

Fig. 6 Schematic diagram of tensile test samples according to DIN 50125 [29]

Table 4 Dimensions of tensile test samples

Parameter according to DIN 50125 [29]	a_0	b_0	B	h	L_0	L_c	L_t	r
Value /mm	8	12	18	40	15	21	125	12

is described briefly at the end of Sect. 3.1. The problem is described in more detail in [28]. For the flow resistivity values of the experimental trailing edges, which need to be determined by expensive measurements, reference is also made to [2, 28].

3 Results and discussion

Measurements of porosity, flow resistivity and mechanical behavior of uniformly rolled samples are shown and discussed. For the discussion, the findings from [1] for PA 200–250 are also used. With this information, reasonable degrees of deformation are identified and realized using the cold rolling technique for the production of graded porous material. At the end of this section, CT scans together with the porosity values resulting from the defect detection of experimental low noise trailing edges are shown. The analyzed TEs are used for testing in an acoustic wind tunnel (AWB at DLR Braunschweig) by Rossignol et al. [2].

3.1 Porosity and flow resistivity

Figure 7 shows the result of the porosity determination of uniformly rolled material for different degrees of deformation. Considering the initial porosity and assuming that the material is compressed only in the thickness direction and does not change its size in the other dimensions, the resulting porosity would be around 20% at $\Delta t/t_0 = 50\%$. However, lengthening occurs in the direction of rolling. At $\Delta t/t_0 = 50\%$ lengthening of samples is approximately 20%. Taking this into account, a porosity value of around 33% has to result, which is in good agreement with the measured values of around 31% porosity. Note that spreading occurs in the direction transverse to the rolling direction. It is only about 1–2% and therefore not taken into account.

One can see that the porosity decreases with the increase in sheet thickness reduction $\Delta t/t_0$. An increase of 10% of $\Delta t/t_0$ is accompanied by a decrease in porosity around 5% except for the last rolling steps from $\Delta t/t_0 = 30$ to 50% where the porosity decreases by a value >5%. When using the true strain instead of the sheet thickness reduction a linear correlation results. This is similar to the results of PA200–250 obtained in [1].

Note that the porosity of all analyzed samples is open. This can exemplary be seen in Fig. 8, where the pores are color coded and the material itself is faded. It can be seen, that there is one main pore volume (red) and a few smaller

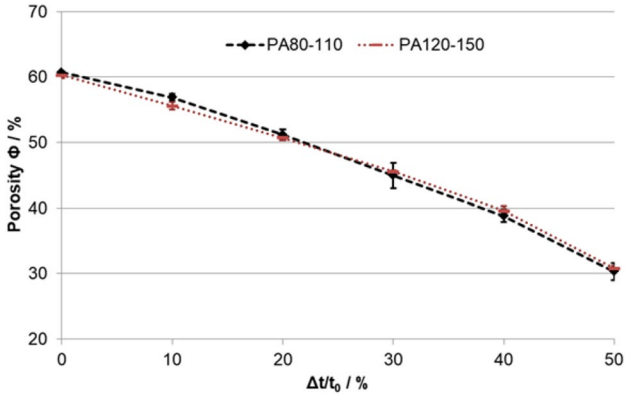

Fig. 7 Porosity of PA 80–110 and PA 120–150 at different degrees of deformation, error bars show standard deviation

pores (blue). The small pores are likely to be connected to the main pore volume, but cut off due to the limited range of the analyzed volume. This result is obtained for the material as received (a and c in Fig. 8), as well as for cold rolled material (b and d in Fig. 8).

The openness of pores shown in Fig. 8 is important for the usage as a low noise trailing edge, since the effect of noise reduction is based on the communication between the flow on the upper and lower wing surface [3–11]. Since the pores are open up to $\Delta t/t_0 = 50\%$, no restrictions for rolling can be derived up to the aforementioned thickness reduction. Note however, that based on the simulations made by Rossian et al. [14, 15] a main goal is to reduce the sudden change from the impermeable, non porous wing surface (wall bound flow) to free flow. So, in purely theoretical terms, it would be favorable that a gradient should change from an almost-solid material or material with almost-closed porosity and almost infinitely high flow resistance (the material should not interact with the flow around the wing at this point) to an open porous material which allows the communication between the upper and lower side of the wing. It has been shown in [1] that such a transition from solid to open porous material is possible. However, the measurements in the acoustic wind tunnel (AWB) carried out within the framework of the research project, which are published elsewhere (compare [2, 9, 12, 13]), have suggested that compression to the point of complete impermeability is not necessary. Therefore the materials were only analyzed up to $\Delta t/t_0 = 50\%$, where open porosity is kept with a major increase in flow resistivity. The openness of pores can likewise be seen in the flow resistivity

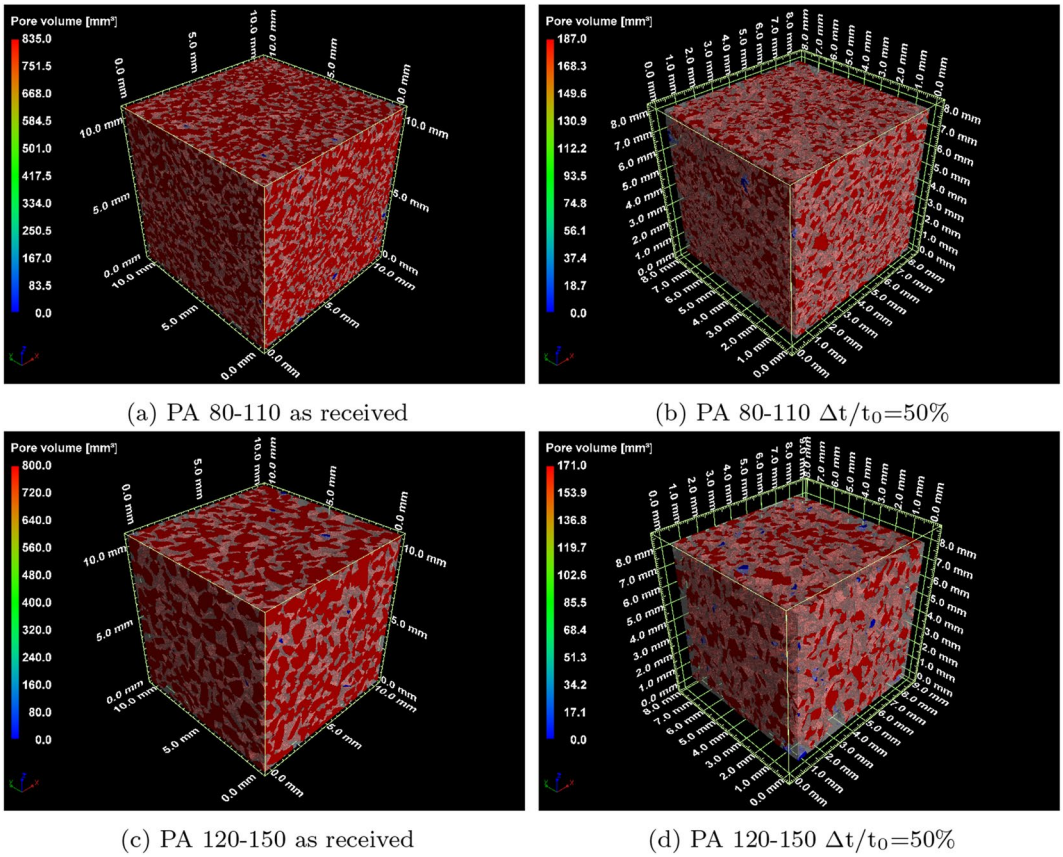

Fig. 8 Computed tomography reconstruction with applied defect detection, pores color coded, material faded

measurements, as the flow resistivity would be infinite for closed pores.

The result of the flow resistivity characterization is shown in Fig. 9. Note, that the flow resistivity is plotted logarithmically to base 10. The overall flow resistivity of PA 120–150 is less than that of PA 80–110. This is due to the increased pore size at constant porosity of PA 120–150 compared to PA 80–110.

For PA 120–150 the increase of flow resistivity is exponential (linear here due to the log-scale), while there is a strange result for PA 80–110. For PA 80–110, there is a minor change in flow resistivity from $\Delta t/t_0 = 20$ to 30%, while the two areas from $\Delta t/t_0 = 0$ to 20% and from $\Delta t/t_0 = 30$ to 50%, considered individually, also show an exponential increase. A similar "anomaly" at 30% is also apparent in the mechanical tests of PA 80–110. That is why it is unlikely to be an effect of inhomogeneous material. Furthermore, comparison with the data from [1] shows that flow resistivity develops similar for PA 120–150 and PA 200–250 (qualitatively). Thus, the "anomaly" at 30% thickness reduction for PA80–110 may be an effect of the reduced pore size of the material leading to a different cold rolling behavior.

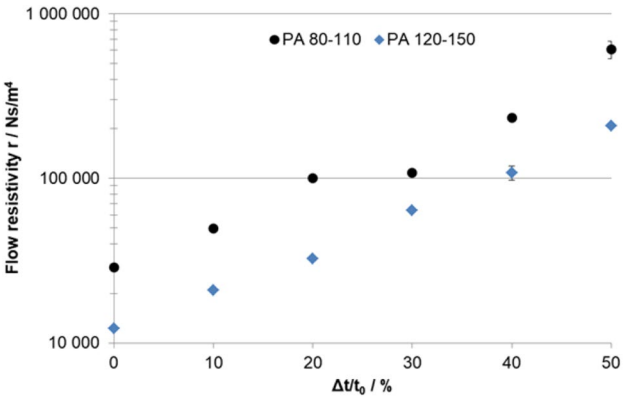

Fig. 9 Flow resistivity of PA80–110 and PA120–150 at different sheet thickness reductions, error bars show standard deviation

One explanation for the measured values could be the formation of cracks on the surface, which may almost completely eliminate the increase of flow resistivity due to compression in the near-surface areas. Such cracks were clearly visible for the rolled PA 80–110 sample (compare Fig. 10a, b), whereas the PA 120–150 sample (compare Fig. 10c, d)

showed only isolated crack initiations. The aspect of crack formation is critically considered when explaining the results of the mechanical behavior.

The specific flow resistivity of experimental trailing edges leading to good aeroacoustic results is in the range of $r \approx$10,000– 150,000 Ns/m^4 [9, 12, 13]. Thus, porous material had to be tailored by rolling in such a way that the resulting gradient lies within this range. Note, that the method for measuring the flow resistivity has an uncertainty of 14% which was not taken into account for the given values. Additionally, the flow resistivity may vary locally due to inhomogeneity. By machining the TEs out, the more dense near surface areas (due to rolling) of the rolled samples are cut off. Furthermore, the size of actual trailing edge of the porous inserts shown in Sect. 3.3 (which are to be used in the wind tunnel experiments) is only about 1.2 mm thick. Taking into account the pore size of the original material, it is clear that there is no longer a representative amount of material volume available here. Pores directly connect the upper and lower side of the wing. That is, why the measurements of the flow resistivity shown here only give a rough guide value for the trailing edge production. A more accurate but expensive method for determining the flow resistivity of experimental trailing edges is described in [28]. For different points of the trailing edge depth, flow resistivity measurement samples are wire cut out of material rolled uniformly. In [28], the difficulties of the procedure are described. As the flow resistivity of the porous inserts should not be the issue here, reference is made at this point to the corresponding publication [2, 28]. Nevertheless, with the values given here, one can see that cold rolling is a suitable process to customize the flow resistivity of porous materials for a given application.

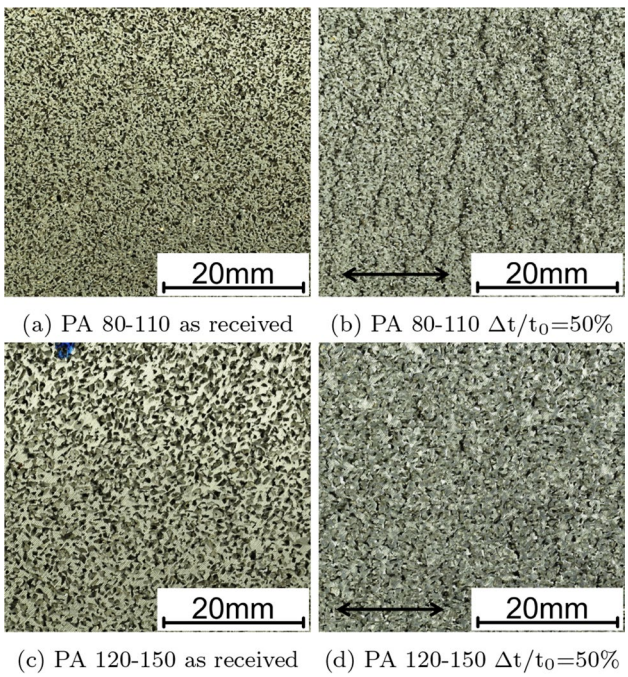

(a) PA 80-110 as received (b) PA 80-110 $\Delta t/t_0$=50%

(c) PA 120-150 as received (d) PA 120-150 $\Delta t/t_0$=50%

Fig. 10 Surface of samples for mechanical testing, as received and after cold rolling at $\Delta t/t_0 = 50\%$, **b**, **d** rolling direction marked

3.2 Mechanical behavior

Figures 11 and 12 show the results of mechanical testing of PA80-110 as received ($\Delta t/t_0 = 0$) and at different sheet thickness reductions. The yield strength is given as a measure of mechanical strength of the porous material. Besides the yield strength, the "corrected" yield strength is given which takes the porosity of the material into account. In other words, for the calculation of the corrected yield strength, the force measured in the tensile tests is related only to an average amount of solid matter within the specimen cross-section. In

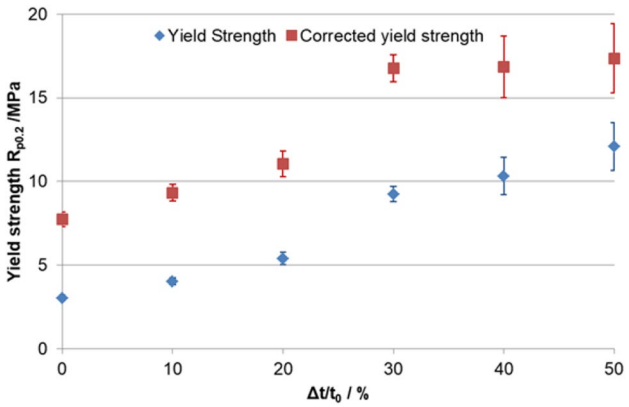

Fig. 11 Yield strength of PA80–110 at different sheet thickness reductions, loading in the direction of rolling, error bars show standard deviation

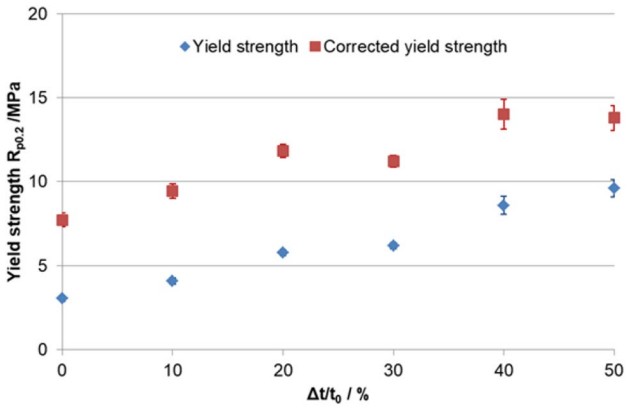

Fig. 12 Yield strength of PA80–110 at different sheet thickness reductions, loading perpendicular to the direction of rolling, error bars show standard deviation

this way, the effect of increasing solid matter in the specimen cross section due to compaction is excluded. As a result, it is easier to identify hardening or damage caused by rolling, as this "geometrical" effect is eliminated.

For loading in the direction of rolling (Fig. 11) a steady increase in yield strength can be seen. However, the scatter of values increases significantly with increasing sheet thickness reduction from $\Delta t/t_0 = 30\%$ on. The corrected yield strength shows an increase as well. The increase can be attributed to work hardening of the material, whereas the increased scatter is an indication of an increase in local damage (compare crack formation in Fig. 10b).

For loading perpendicular to the direction of rolling (Fig. 12), the results are similar. There is an overall increase in yield strength as well as in the corrected yield strength. Except at $\Delta t/t_0 = 30\%$ the yield strength in the perpendicular direction is almost the same as the yield strength at $\Delta t/t_0 = 20\%$, thus the corrected yield strength is decreasing (Fig. 12). This is a clear indication of damage due to rolling, but it contradicts the results of the tensile tests in the rolling direction (Fig. 11). Figure 11 shows a clear increase in both the yield strength and the corrected yield strength.

The fact that damage occurs is shown in Fig. 10. However, the tensile test specimens are worked out of the mid of the material. Looking at a thickness reduction of 30%, the resulting thickness of the material after rolling is around 14 mm. The thickness of the tensile test samples was around 8 mm. That means, there are 3 mm of material on each side to the surface of the rolled samples, where cracks do not affect the mechanical test results. The way the cracks appear on the surface, they do not extend 3 mm into the material. However it is possible that cracks were forming on the inside of the material as well.

The question that arises at this point is therefore why the tensile tests perpendicular to the rolling direction clearly show damage that is not clearly evident from the tests in the rolling direction. Considering that the cracks shown in Fig. 10b are perpendicular to the rolling direction, these cracks should be much more damaging when exposed to a tensile load in the rolling direction than when exposed to a tensile load transverse to the rolling direction. So far, this effect has not been understood. The study of the damage behavior by tensile testing combined with CT-analysis will clarify this aspect. The corresponding measurements are still under evaluation.

At this point an important remark must be made. The thickness of the tensile test specimens is 8 mm, which is still thicker than the maximum thickness of the trailing edges, which is around 6.5 mm. If the damage caused by cracks is indeed only on the surface, it is therefore acceptable that these cracks are not fully considered in the tensile tests. The tensile tests carried out have the desired informative value for the intended application as a trailing edge.

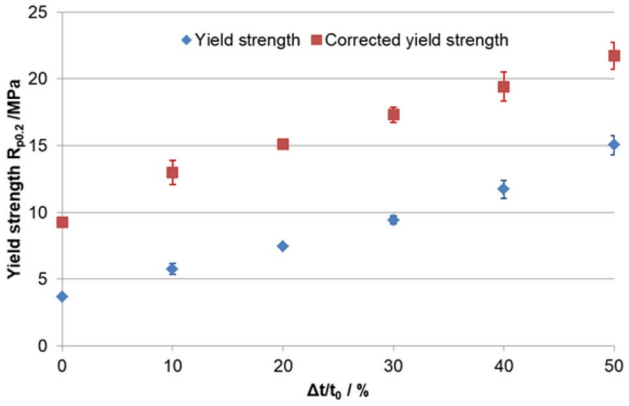

Fig. 13 Yield strength of PA 120–150 at different sheet thickness reductions, loading in the direction of rolling, error bars show standard deviation

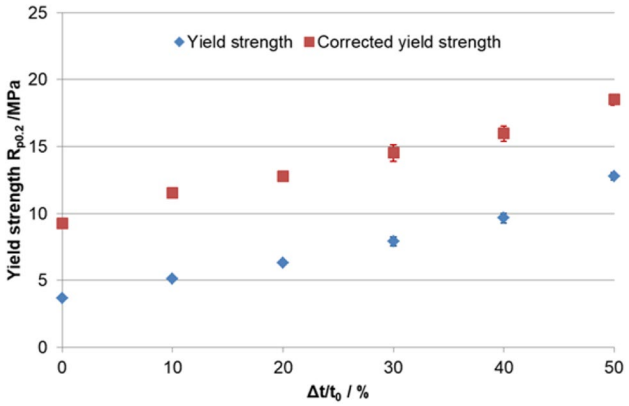

Fig. 14 Yield strength of PA 120–150 at different sheet thickness reductions, loading perpendicular to the direction of rolling, error bars show standard deviation

Figures 13 and 14 show the results of mechanical testing of PA 120–150. In both loading directions, the yield strength is constantly increasing with an increase in the referenced sheet thickness reduction. This is also valid for the corrected yield strength. Comparing Figs. 13 and 14 one can see that the yield strength is slightly higher for the rolled material in case the load during tensile testing is applied in the direction of rolling (Fig. 13). This can be attributed to the greater elongation of the material in the rolling direction, which leads to an increase in work hardening effects in this direction.

Based on those results, there are no limitations regarding the sheet thickness reduction in the range of 0–50% for PA120–150. No degradation of the material due to cold rolling could be detected.

Besides, rolling can even produce a more favorable combination of the material properties yield strength and flow

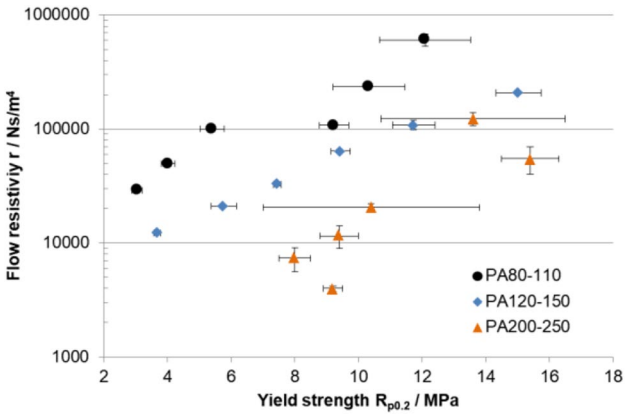

Fig. 15 Scatter plot of yield strength and flow resistivity of PA80–110, PA120–150 and PA200–250 [1] as received and cold rolled, error bars show standard deviation

resistivity. Looking at the flow resistivity of PA 80–110 as received, it is about 30 000 Ns/m^4 for the material used here. The yield strength of the material as received is about 3 MPa. The same flow resistivity can be achieved with cold rolled PA 120–150 at a referenced sheet thickness reduction between 10 and 20%. However, the yield strength of 5–6 MPa of such a material would be almost twice as high as that of the comparable PA 80–110. This can be seen very well in the scatter plot for the yield strength and flow resistivity in Fig. 15. With regards to the aeroacoustic behavior, the influence of the increased pore size and therefore the increased surface roughness needs to be considered.

Comparing the results shown here with the results for PA200-250 in [1], one can see a systematic trend in material strength for the material as received. The strength seems to increase with increasing pore size, compare Fig. 15, where data for all analyzed materials is given. This is surprising given the self-similar structure with the same or similar pore shape and porosity. One possible cause is the ratio of wall thickness to grain size of the material. It is planned to study this aspect by metallographic analysis. Since work hardening has occurred for both materials in this study, it is also necessary to investigate why work hardening was not clearly found in [1] for PA 200-250.

3.3 Experimental low noise trailing edges

The manufacturing process of experimental trailing edges is described in Sect. 2.2. In [1], a reference experimental TE out of PA 80-110 as well as experimental TEs out of PA 200-250 (made out of material as received and cold rolled) are shown. In the following, additional experimental trailing edges for aeroacoustic measurements in the acoustic wind tunnel of the DLR Braunschweig are shown. In particular, it is described how the porosity of the individual trailing edges was adjusted by the cold rolling process and which differences between the different materials and different rolling states can be recognized in computed tomography cross-sections.

Table 5 shows the determined porosity values for seven different experimental trailing edges. Comparing TEs that were rolled with the standard gradient with the values of TEs from the corresponding material (as received) it becomes apparent that no linear porosity decrease has taken place over the length of the TE. As described before [1, 28], deformation localization occurs in the near-surface

Table 5 Porosity of experimental trailing edges, measured in Region 1-6 (compare Fig. 5)

TE no.	Material used	Porosity /% of no. of region of interest					
		1	2	3	4	5	6
I	PA 80–110 (Fig. 18a)[a] as received	52	52	53	52	52	50
II	PA 80–110 (Fig. 18b)[a]						
	$\Delta t/t_0$ = 10–50%	52	53	49	43	36	28
III	PA 120–150 (Fig. 18c)						
	as received (Batch18)	63	63	62	63	62	61
IV	PA 120–150 (Fig. 18e)						
	as received (Batch17)	57	55	57	57	57	56
V	PA 120–150 (Fig. 18d)						
	$\Delta t/t_0$ = 0 – 30% (Batch18)	61	59	60	59	56	50
VI	PA 120–150 (Fig. 18f)						
	$\Delta t/t_0$ = 10–50% (Batch17)	51	48	44	39	32	26
VII	PA 120–150 (Fig. 18g)						
	$\Delta t/t_0$ = 10–67.5% (Batch17)	51	48	43	35	27	16

[a]The TEs out of PA80-110 are made out of a different batch than the one shown in [1]. These batches have a very different pore geometry resulting in different properties. According to the manufacturer, the production process was changed

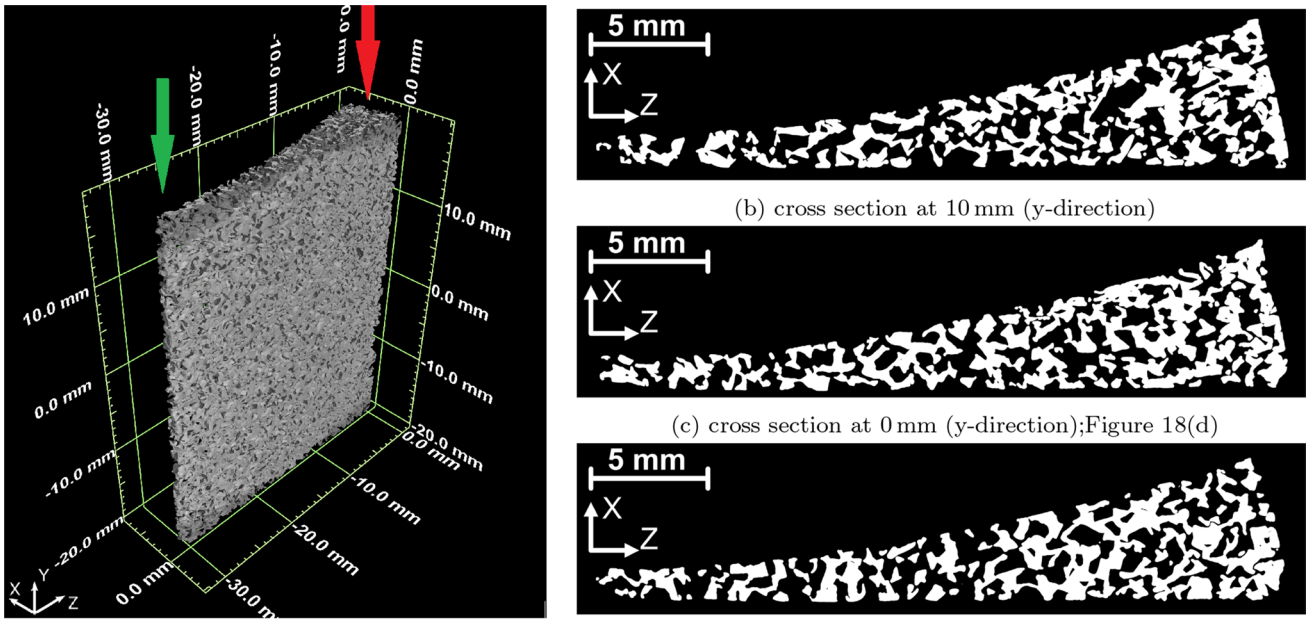

Fig. 16 Section of an experimental trailing edge made of cold rolled PA120–150 with a gradient in thickness reduction from 0 to 30% (No. V)

areas at small values of referenced sheet thickness reductions. Since the trailing edges are machined out of the middle of the material, the influence of rolling is comparatively small for small values of referenced sheet thickness reductions. This effect is particularly noticeable in ROI 1, 2 (and 3) where the thickness reductions are small and the trailing edge thickness is correspondingly small (see green arrow Fig. 16). The area of the TE only consists of a narrow area out of the middle of the rolled material.

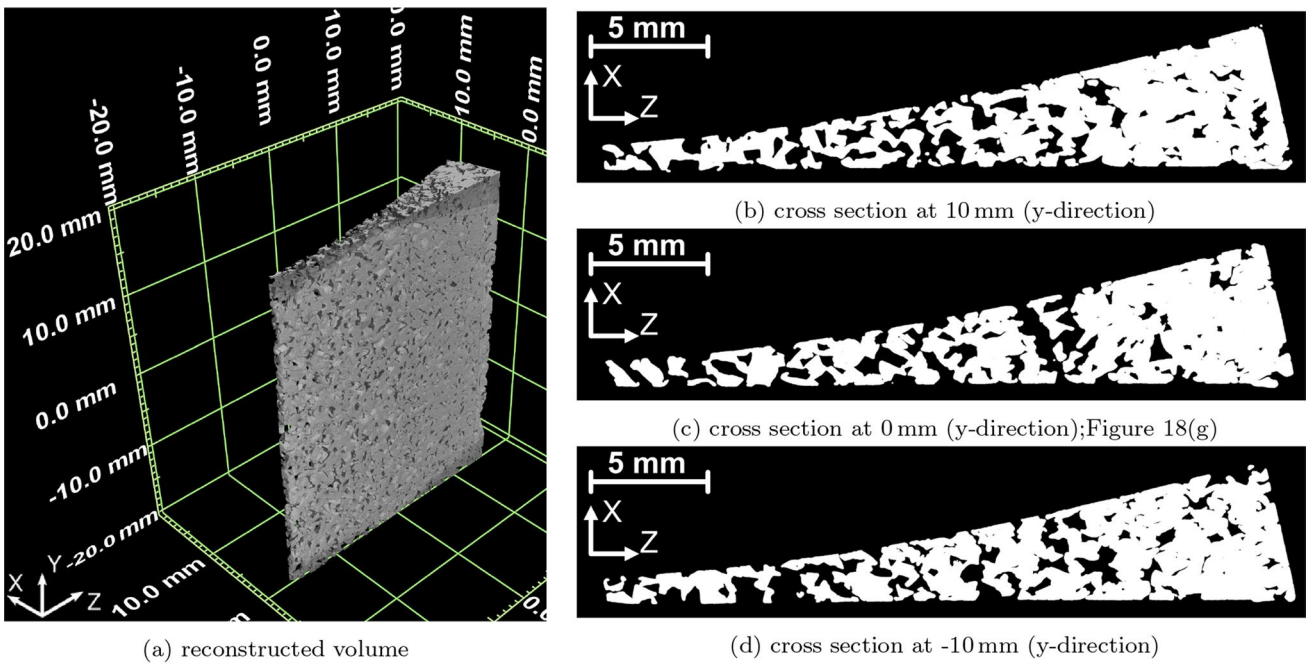

Fig. 17 Section of an experimental trailing edge made of cold rolled PA120–150 with a gradient in thickness reduction from 10 to 67.5% (No. VII)

(a) PA80-110 as received (No.I)

(b) PA80-110 "standard gradient" (No.II)

(c) PA120-150 as received (Batch18) (No.III)

(d) PA120-150 "light gradient" (Batch18) (No.V)

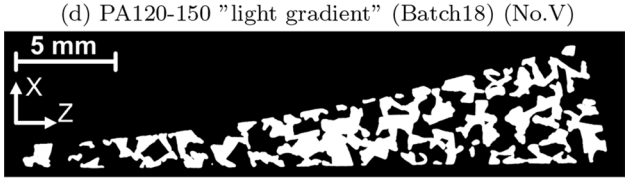

(e) PA120-150 as received (Batch17) (No.IV)

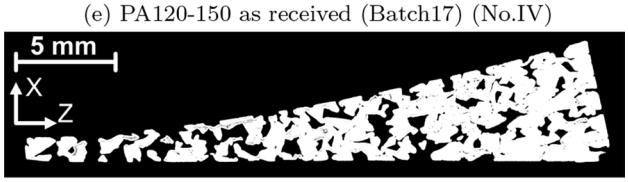

(f) PA120-150 "standard gradient" (Batch17) (No.VI)

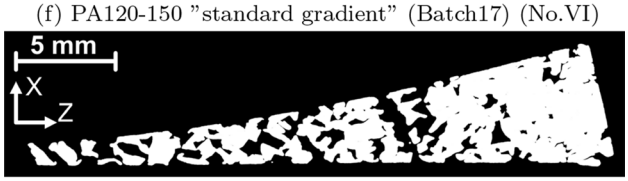

(g) PA120-150 "maximum gradient" (Batch17) (No.VII)

Fig. 18 Cross sections of different experimental trailing edges

Apart from that, one can see that the gradients set during rolling are very clearly reflected in the porosity of the trailing edges (Table 5 No. II, V–VII). Since different gradients have been investigated with PA120-150, they will be described in the following. For this purpose, Figs. 16a and 17a show the computed tomography reconstructions of TE sections. On the one hand a TE made out of material rolled with the light gradient (Fig. 16, Table 1) and on the other hand a TE made out of material rolled with the maximum gradient (Fig. 17, Table 3) is shown. Figure 16a shows hardly any change in the pore structure on the surface. Close to the point of attachment (red arrow) respectively in ROI 6 and 5 a decrease in porosity can be assumed. This decrease is clearly shown in the porosity measurements (Table 5 No. V). For the TE out of cold rolled material with the "maximum" gradient the decrease in porosity can clearly be seen comparing ROI 1 with ROI 6 in Fig. 17a. This is also reflected in the porosity measurements (Table 5 No. VII). Comparing the porosity of ROI 1 in No.V and No.VII a difference of around 10% is measured. This difference can be seen between Figs. 16a and 17a, too.

Due to the limited analyzability of the three-dimensional material models, cross sectional images of the computed tomography measurements are shown in Figs. 16b–d, 17b–d and for all TEs in Fig. 18. For reasons of space, three cross sectional images are given only for No. V and No. VII. For the other TEs only one representative cross-sectional image is shown.

When looking at such cross sectional images, the reader should be aware that the images can easily be misleading. Even if no connection between the suction and pressure sides can be seen in the cross sectional image, the pores naturally continue to extend outside the sectional planes, so that there surely is a connection between the suction and pressure sides.

The previously described difference of the trailing edges made out of material rolled with the "light" gradient (Figs. 16b–d, 18d) and "maximum" gradient (Figs. 17b–d, 18g) in thickness reduction can also be seen very distinctly in the cross sections of the computed tomography scans.

Comparing Fig. 18c and d one can see that the size of pores and the porosity is almost the same, except for the point of attachment (right hand side of cross-sections). There, Fig. 18d shows less porosity and smaller pores compared to the starting material in Fig. 18c. Comparing Fig. 18e, g, on the contrary, a much more distinct difference is apparent. On the left hand side of the cross sections, the difference in porosity and pore size does not seem to be major, although the difference in porosity according to measurement (Table 5) is 6 %. However, a major difference can be seen when looking at the point of attachment (right hand side of cross-sections). There, in Fig. 18g pores are a lot smaller than those of Fig. 18e. Furthermore, the pores seem not to be open anymore, with porosity being close to zero (though porosity is still 16 % according to measurement Table 5). From the aeroacoustic requirements, the aim of a graded transition from solid to porous material was best achieved in this case.

Looking at the cross section of Fig. 18g (compared to c–f), however, it also becomes clear that the effective length over which the material is porous may be reduced. Thus,

the length over which the material can achieve its actual effect is reduced, which certainly has an influence on the aeroacoustic behavior. Nevertheless, the demands made by [9, 12–14] for porous materials can be met. The aeroacoustic measurements [2] did not allow a clear quantification of the effect of porous material rolled with a gradient in thickness reduction. They seem to influence mainly the low-frequency part and seem to provide only slightly better noise reductions [2]. Now further adjustments that have to be made for highly efficient experimental low noise trailing edges have to be concluded. Within the experiments shown here, it has become clear that different gradients can be generated by cold rolling.

4 Conclusions

The results of this study show that the porosity and flow resistivity of porous materials can be effectively adjusted by cold rolling. The porosity decreases almost linearly with the increase of the related sheet thickness reduction. The flow resistivity, on the other hand, increases exponentially. It is also shown that there are no limitations of the rollability up to a referenced sheet thickness reduction of 50% with regard to the mechanical stability of the material. With regard to PA80-110, it has been shown that rolling does cause damage which does not negatively influence the mechanical properties compared to the starting material, but has a considerable influence on the flow resistivity. This aspect is to be further researched by additional rolling experiments combined with high resolution computed tomography scanning.

Comparing the results of this study with those of PA200-250 found in [1] a systematic trend can be derived. Despite self similar structures, materials with larger pores and ligaments at the same porosity and pore shape appear to be superior to the mechanical properties of materials with finer pores. The reason for this could be the ratio of ligament size to grain size, which is presumably not constant. To investigate this, analyzation of the materials with metallographic methods will be done.

The investigations show that there may be variations in the starting material which may be intensified by rolling. This is shown in the increased scatter values in the tensile tests as well as in the flow resistivity measurements for high degrees of deformation. The influence of this scatter onto the aeroacoustic behavior still needs to be determined. So far, it can only be concluded that the requirements from [9, 14] are met with certain deviations and that the rolling process which is used allows to produce experimental porous trailing edges at reasonable costs.

The rolling process described in [1] was successfully carried out on porous materials with other filter fineness. Experimental trailing edges of rolled materials with different gradients in thickness reduction were presented and analyzed, showing the versatility of the new rolling technique. The aeroacoustic behaviour of these materials was partly characterized by [2]. Only a slight advantage of using porous materials with a porosity gradient could be identified. Further investigations need to be performed, to examine whether the gradients investigated lie within the acoustically relevant range and to identify adjustments that need to be made.

Acknowledgements Funded by the Deutsche Forschungsgemeinschaft (DFG, German Research Foundation)—Projektnummer 133733460—SFB880 (CRC880) We wish to acknowledge the help provided by Lennart Rossian from the DLR Braunschweig who provided Fig. 1 as well as input with regards to the aeroacoustics. We also wish to acknowledge the help provided by Christopher Blech from the Institute for Acoustics of TU Braunschweig, who carries out the flow resistivity measurements within the framework of the CRC880.

Funding Open Access funding enabled and organized by Projekt DEAL.

Declarations

Conflict of interest The authors declare that they have no conflict of interest.

References

1. Tychsen, J., Lippitz, N., Rösler, J.: Modification of porous aluminum by cold rolling for low-noise trailing edge applications. Metals **8**, 598 (2018). https://doi.org/10.3390/met8080598
2. Rossignol, K.-S., et al.: Experimental investigation of porous materials for trailing-edge noise reduction. Int. J. Aeroacoust. **19**, 365–384 (2020). https://doi.org/10.1177/1475472X20954421
3. Bohn, A.J.: Edge noise attenuation by porousedge extensions. In: 14th Aerospace Sciences Meeting. (1976), p. 80
4. Showkat, A., Syamir, A., Azarpeyvand, M., Roberto Ilàrio da Silva, C.: Trailingedge flow and noise control using porous treatments. J. Fluid Mech. **850**, 83–119 (2018). https://doi.org/10.1017/jfm.2018.430
5. Kisil, A., Ayton, L.J.: Aerodynamic noise from rigid trailing edges with finite porous extensions. J Fluid Mech. **836**, 117–144 (2018). https://doi.org/10.1017/jfm.2017.782
6. Koh, S.R., Meinke, M., Schröder, W.: Numerical analysis of the impact of permeability on trailing-edge noise. J. Sound Vib. **421**, 348-376 (2018). ISSN: 0022-460X. https://doi.org/10.1016/j.jsv.

2018.02.017 . http://www.sciencedirect.com/science/article/pii/S0022460X1830107X
7. Rubio, C., Alejandro., A, Francesco., Ragni, D.: On the role of the flow permeability of metal foams on trailing edge noise reduction. In: 2018 AIAA/CEAS Aeroacoustics Conference, p. 2964 (2018)
8. Carpio, A.R., et al.: Experimental characterization of the turbulent boundary layer over a porous trailing edge for noise abatement. J. Sound Vib. **443**, 537–558 (2019). ISSN: 0022-460X. https://doi.org/10.1016/j.jsv.2018.12.010 . http://www.sciencedirect.com/science/article/pii/S0022460X18308277
9. Herr, M., et al.: Specification of porous materials for low-noise trailing-edge applications. In: 20th AIAA/CEAS Aeroacoustics Conference. (2014). ISBN: 9781624102851
10. Vathylakis, A., Chong, T.P., Joseph, P.F.: Poro-serrated trailing-edge devices for airfoil self-noise reduction. AIAA J. **53**, 3379–3394 (2015)
11. Lockard, D.P., Lilley, G.M.: The airframe noise reduction challenge. NASA Technical Reports Server (2004)
12. Delfs, J., et al.: FB 880: aeroacoustic research for low noise take-off and landing. CEAS Aeronaut. J. (2014). ISSN: 18695582. https://doi.org/10.1007/s13272-014-0115-2
13. Delfs, J.W., et al.: Aircraft and technology for low noise short take-off and landing. In: 35th AIAA applied aerodynamics conference, 2017. (2017). ISBN: 9781624105012 . https://doi.org/10.2514/6.2017-3558
14. Rossian, L., Ewert, R., Delfs, J.W.: Prediction of airfoil trailing edge noise reduction by application of complex porous material. In: Notes on Numerical Fluid Mechanics and Multidisciplinary Design, vol. 136, pp. 647–657 (2018). ISBN: 9783319645186 . 10.1007/ 978-3-319-64519-3 _58
15. Rossian, L.: Minderung der Schallabstrahlung von Hochauftriebssystemen mittels aeroakustisch wirksamer poröser Materialien in Verbindung mit aktiver Strömungskontrolle. PhD thesis. DLR, (2019)
16. Rossian, L., Ewert, R., Delfs, J.: Advances in numerical simulation of trailing edge noise reduction by porous materials. In: Rolf, R. and Richard, S. (eds.) SFB 880 —Fundamentals of highlift for future commercial aircraft. Berichte aus der Luft- und Raumfahrttechnik. TU Braunschweig Campus Forschungsflughafen, Braunschweig, pp. 1–10 (2017). ISBN: 978-3-928628-90-7
17. Rubio, C., Alejandro. et al.: Mechanisms of broadband noise generation on metal foam edges. Phys. Fluids. (2019). ISSN: 10706631. https://doi.org/10.1063/1.5121248
18. Schulze, J., Sesterhenn, J.: Optimal distribution of porous media to reduce trailing edge noise. Computers Fluids, **78**, 41–53 (2013). ISSN: 00457930. https://doi.org/10.1016/j.compfluid.2011.12.022
19. Fassmann, B.W., et al.: Prediction of porous trailing edge noise reduction via acoustic perturbation equations and volume averaging. In: 21st AIAA/CEAS Aeroacoustics Conference, p. 2525 (2015)
20. Rossian, L., et al.: Prediction of porous trailing edge noise reduction using acoustic jump-conditions at porous interfaces. In: 22nd AIAA/ CEAS aeroacoustics conference, p. 2920 (2016)
21. Devenport, W.J., et al.: Measurements of roughness noise. J. Sound Vib. **330**, 4250–4273 (2011). ISSN: 0022- 460X. https://doi.org/10.1016/j.jsv.2011.03.017 . http://www.sciencedirect.com/science/article/pii/S0022460X11001970
22. Sarradj, E., Geyer, T.: Symbolic regression modeling of noise generation at porous airfoils. J. Sound Vib. **333**, 3189–3202 (2014). ISSN: 0022-460X. https://doi.org/10.1016/j.jsv.2014.02.037 . http://www.sciencedirect.com/science/article/pii/S0022460X14001783
23. Geyer, T.F., Sarradj, E.: Trailing edge noise of partially porous airfoils. In: 20th AIAA/CEAS aeroacoustics conference., p. 3039 (2014)
24. Fritz Geyer, T., Sarradj, E.: Self noise reduction and aerodynamics of airfoils with porous trailing edges. Acoustics. **1**, 393–409 (2019)
25. Erman Tekkaya, A., Homberg, W., Brosius, A.: 60 Excellent inventions in metal forming. Springer, Berlin (2015)
26. Hauger, A., Muhr, T., Kopp, R.: Flexible rolling of tailor rolled blanks. In: Stahl und Eisen 126.5 , pp. 21–23 (2006)
27. Lippitz, N.: Poröse Materialien zur Reduzierung von Hinterkantenschall an Flugzeugflügeln. Dissertation. Technische Universität Braunschweig, (2017)
28. Tychsen, J., Rösler, J.: Production and characterization of porous materials with customized acoustic and mechanical properties. In: Fundamentals of high lift for future civil aircraft, pp. 497-512. Springer, Berlin (2020)
29. Deutsches Institut für Normung: Prüfung metallischer Werkstoffe: Zugproben = Testing of metallic materials. Tensile test pieces, Berlin (2016)
30. Harders, H.: Ermüdung von Aluminiumschaum: Braunschweig, Techn. Univ., Diss., 2005. Braunschweig and Tönning: Univ.-Bibl and Der Andere Verlag, 2005. ISBN: 3899594002 . http://opus.tu-bs.de/opus/volltexte/ 2005/810
31. Deutsches Institut für Normung. Acoustics, Materials for Acoustical Applications; Determination of Airflow Resistance German Version DIN EN 29053:1993-05. Berlin, Germany, (1993)
32. Blech, C. et al.: Origin and prediction of cabin noise due to structure-borne sound. In: Rolf, R., Richard, S. (eds.) SFB 880—fundamentals of high-lift for future commercial aircraft. Ed. by. Berichte aus der Luft- und Raumfahrttechnik. Braunschweig: TU Braunschweig Campus Forschungsflughafen, (2017). ISBN: 978-3-928628-90-7